Proceedings of Fifth International Conference on **Enhanced, Compact and Ultra-Compact Heat Exchangers: Science, Engineering and Technology**, Eds. R.K. Shah, M. Ishizuka, T.M. Rudy, and V.V. Wadekar, Engineering Conferences International, Hoboken, NJ, USA, September 2005.

CHE2005 – 53

THE MANUFACTURE OF MICRO CROSS-FLOW HEAT EXCHANGERS BY SELECTIVE LASER MELTING

S. Tsopanos[1], C. J. Sutcliffe[2], I. Owen[3]

[1]The University of Liverpool, Liverpool, UK; sozos@liv.ac.uk
[2] The University of Liverpool, Liverpool, UK; c.j.Sutcliffe@liv.ac.uk
[3] The University of Liverpool, Liverpool, UK; I.Owen@liv.ac.uk

ABSTRACT

Selective Laser Melting, a layer-based Solid Freeform Fabrication process, has been used to fabricate micro cross-flow heat exchangers from 316L Stainless Steel powder. Selective Laser Melting (SLM) technology is based on automated layer additive fabrication and represents a departure from the existing manufacturing techniques for micro heat exchangers, such as precision machining, chemical etching and diffusion bonding. The Selective Laser Melting technique uses a 100-Watt Ytterbium fibre laser to fully melt a pre-deposited layer of a single component metallic powder onto a substrate according to a computer-generated pattern. By successive powder deposition of these layers at 50 microns thickness, fully dense, micro cross-flow heat exchangers have been built. Micro heat exchangers involving heat transfer and flow in microchannels have found applications in highly specialised areas such as microelectronics cooling, aerospace, microfabricated fluidic systems, and biomedical processes where lightweight, small volume heat exchangers are required. The Selective Laser Melting technique can provide custom-designed micro heat exchangers fabricated from stainless steel or copper in special geometries not possible by any other manufacturing method. SLM allows the heat exchanger plate wall thickness, as well as channel dimensions and geometries to be carefully controlled in the range of 150 to 750 microns with a typical surface roughness, Ra, of 15 microns. The prototype micro heat exchanger tested in this study provided an overall heat transfer coefficient 2.22 kW/m^{2}K, which corresponds to a volumetric heat transfer coefficient of 3.14 MW/m^{3}K, under very moderate design and operating conditions.

INTRODUCTION

The significance of microchannels lies in their high heat transfer coefficient and significant potential for decreasing the size of heat exchangers. As microchannels offer an increased heat transfer surface area and a large surface-to-volume ratio, providing a much higher heat transfer per unit volume than channels of conventional size. This characteristic allows heat exchangers to become compact and lightweight. From the literature it is apparent that research conducted into the performance of micro heat exchangers tends to use in the first instance micro cross flow heat exchangers of the configuration shown in Fig. 1.

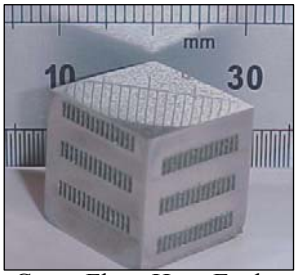

Figure 1: Micro Cross Flow Heat Exchanger by Selective Laser Melting

The research reported in this paper introduces the fabrication of micro cross-flow heat exchangers by SLM, an example of which can be seen in Figure 1.

Tuckermann and Peace et al. (1981) were perhaps the first to investigate micro heat transfer by fabricating and testing a high performance water-cooled heat sink. In the device, heat generated by the microelectronics components is removed by a coolant flowing through channels located as close as possible to the heat source. The microchannel configuration was manufactured using an orientation-dependent etch (KOH) to a depth of 300μm with channel and fin width of 50μm in silicon wafers of 400μm thickness. Heat exchanger geometries here developed by stacking silicon wafers and they were tested with water as the working fluid. A heat flux of 790 W/cm^2 was measured with a temperature difference of 71 ^{0}C and thermal resistances as low as 0.09 ^{0}C/W were achieved over a surface area of 1cm^2.

Cross and Ramshaw et al. (1986) studied the performance of micro cross-flow heat exchangers with channels 300 μm deep and 400 μm wide, that were manufactured using photo-etching of corrugated titanium plates. The micro heat exchangers exhibited volumetric and overall heat transfer coefficients as high as 7 MW/m^{3}K and 4 kW/m^{2}K, respectively. These performance figures emphasized the attraction of laminar flow heat exchangers coupled with micro channels.

A mechanical method, which has been applied to the manufacturing of micro channel heat exchangers, was developed by Bier et al. (1990). In this case, patterns were generated by precision cutting of foils with profiled microdiamonds followed by joining stacked layers of foils to create the micro heat exchanger body. Electron beam welding, laser welding and diffusion bonding were used to join the stacked elements within the heat exchanger to produce cross-flow micro heat exchangers from aluminum alloy, copper, stainless steel and titanium. These geometries were subsequently tested with water as the working fluid. The heat transfer results were presented for a micro heat exchanger made of copper with water as the working fluid. These showed that it was possible to transfer in a cubic volume of 1 cm^3 thermal powers of about 20 kW at mean logarithmic differential temperature of 60 ^{0}C. Channels 1 cm long with a characteristic diameter of 88μm, achieved an extremely high volumetric heat transfer coefficient of 234 MW/m^{3}K and an overall heat transfer coefficient of 22.8 kW/m^{2}K with both water streams experiencing pressure drops of 4.7 bar.

The machining of thin metal foils with profiled diamond cutting tools and bonding them by a vacuum diffusion process to form a cross-flow plate type micro heat exchanger was investigated by Friedrich and Kang et al. (1994). They developed a copper cross-flow micro heat exchanger with trapezoidal channels of 100 μm hydraulic diameter, exhibiting a volumetric heat transfer coefficient of 45 MW/m^{3}K and an overall heat transfer coefficient of 6 kW/m^{2}K.

Fluid flow and forced convection heat transfer in micro heat exchangers with both micro channels and porous media were investigated experimentally by Jiang et al. (2001). It was shown that the heat transfer performance of the micro heat exchanger using porous media is better than that of the one using micro channels, but the pressure drop of the former is much larger. The maximum volumetric heat transfer coefficients were 86.3 and 38.5 MW/m^{3}K and pressure drops were 4.66 and 0.7 bar for the porous media and the microchannel device respectively. Considering both the heat transfer and pressure drop characteristics of the devices, the deep microchannel design was found to offer a better overall performance.

The dimensions, physical characteristics and performances of different cross flow micro heat exchangers investigated previously are listed in Table 1. Most micro channel heat sinks use deep channels, with an aspect ratio greater than one, while micro channel heat exchangers usually have shallow channels, and aspect ratio of less than one [Jiang et al. (2001)]. It can also be seen that the overall heat transfer coefficient improves as the channel width decreases and channel depth increases. In general, it appears that the smaller the hydraulic diameter of the channels the better the overall heat transfer performance of the device.

The fabrication methods presented in Table 1 can produce high thermal performance micro devices. However, they require multiple, expensive and inflexible processes to create devices, for instance, for optical lithography. These processes include mask-making, photoresist coating and heating, exposing, etching and cleaning, whilst for precision micro machining specialized tools, vibration isolation, micro control, and thermal stability are required. The Selective Laser Melting technique presented in this paper can deliver functional micro heat exchangers rapidly, in very complex geometries with very few of the complications mentioned above.

Table 1: Dimensions and thermal performance of micro heat exchangers.

References	W_c (mm)	h_c (mm)	D_h(mm)	h_c/W_c	U (kW/(m^{2}K))	U_V (MW/(m^{3}K))	Fluids/ Flowrate (l/min)	Manufacturing method
Tuckerman et al. (1981)	0.05	0.3-0.32	0.086	6	21.2		Water 0.3-0.5	Silicon Etching
Cross et al. (1986)	0.4	0.3	0.343	0.75	4.0	7	Water 2.16	Copper, photo etched plates
Bier et al. (1990)	0.1	0.078	0.088	0.78	22.8	324	Water max.12.5	Precision machining
Friedrich et al. (1994)	0.26	0.08	0.122	0.3	6.44	33.3-44.3	Water 0.84-2.7	Diamond machining,
Jiang et al. (2001) MCHE/MPHE	0.2	0.6	0.3	3	13.3/60.4	38.5/86.3	Water 20.4/4.02	Copper plates, wire cutting
S.W. Kang et al. (2002)	0.04	0.2	0.067	5	24.7	188.5	Water	Silicon etching

DESIGN

Compared with conventional heat exchangers, the main advantage of micro heat exchangers is their high heat transfer area per unit volume and hence the high overall heat transfer coefficient per unit volume. Micro channel heat exchangers are the most common type of micro heat exchangers and generally consist of many channels fabricated from thin foils of silicon or metallic materials. Typical cross-flow micro heat exchanger geometries use

stacked micro channel plates alternating at 90°. A disadvantage of the stacking method is the cost and the time involved in manufacturing and bonding together the numerous plates. Fluids with similar properties are typically used as the heat transfer media and this allows identical stacked plates to be used, making the fabrication process less complicated. As the channels on both sides are of the same geometry, as are the mass flow rates and heat transfer conditions, it is reasonable to assume that heat transfer coefficients are almost the same on both sides, this makes the collection of data more straightforward. A basic schematic of this type of micro cross-flow heat exchanger is shown in Figure 2. The research for this type of heat exchanger has so far only appeared to involve heat transfer between similar fluids. However using SLM as a novel manufacturing process can offer greater flexibility, introducing different patterns and dimensions in each layer without causing problems in the manufacturing method as no special tooling is required and no extension in the manufacturing time will occur.

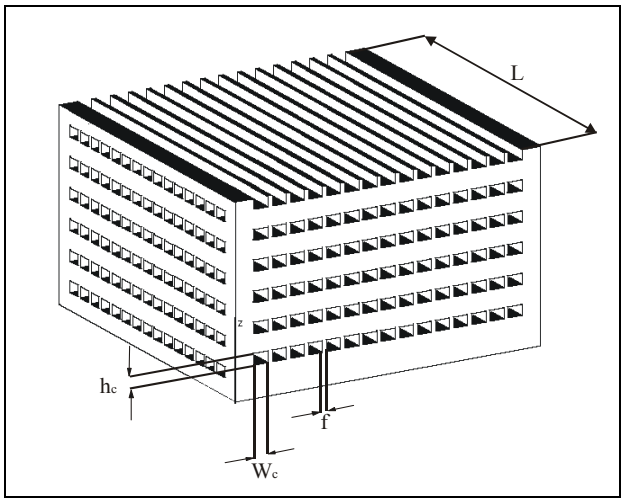

Figure 2: Basic Schematic of a Cross Flow Heat Exchanger.

The micro cross flow heat exchangers fabricated so far by Selective Laser Melting have been of a conservative design so that manufacturing and operating parameters could be easily identified and compared with previous work. As such this paper should be considered as the first step on the development of this type of thermal geometry.

FABRICATION

Selective Laser Melting

Microchannels can be conventionally manufactured as explained earlier by using various techniques, such as X-ray lithography (LIGA), silicon etching, chemical etching, ion beam machining, diamond machining, precision mechanical sawing or wire machining. The fabrication method used here is Selective Laser Melting (SLM), a layer addition Solid Freeform Fabrication (SFF) technique. In the SLM process a succession of individual part cross sections are created from powdered materials by melting them with a 100 W Ytterbium Fibre Laser. A layer-by-layer representation of a micro heat exchanger is shown in Figure 3. The fact that SFF technologies are based on automated additive fabrication means that they represent a complete departure from conventional heat exchanger manufacturing techniques.

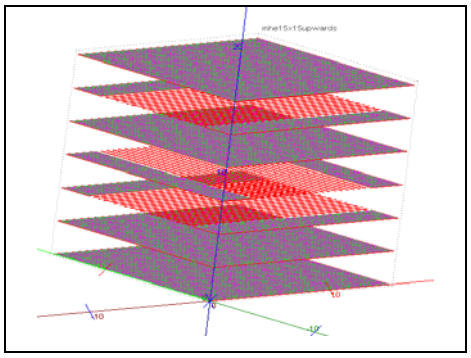

Figure 3: Layer slicing example.

The file format for the three dimensional CAD input to the system is known as the STL (STereoLithography) [Jacobs, 1996] format and is the most standard file format for data input in the Rapid Manufacturing industry. Figure 4 shows a schematic of all the progress stages and information workflow for preparing and pre-processing the data involved in Rapid Manufacturing.

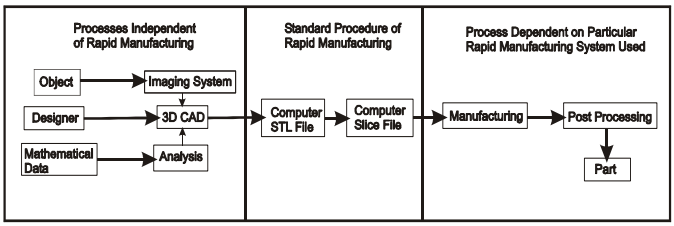

Figure 4: Basis of Rapid Manufacturing Processes, (Murphy et al. 1995).

Selective Laser Melting uses single component powder particles, which are fully melted by a laser beam as it draws the design over the powder bed. This molten material then solidifies and the resultant structure is fully dense. SLM is similar to Selective Laser Sintering (SLS) as both are based on similar concepts. The main difference is the partial melting of the powder in SLS and full melting in SLM. SLS uses base metal powders coated with polymer binder components, or a combination of low and high melting point alloys, for that reason SLS processed parts are not fully dense and hence have relatively low strength [Agarwala et al. (1995)] requiring post processing before being of any use. As shown in Figure 5, a layer of powder is pre-deposited onto the previous layer or the substrate and

spread uniformly by a wiper. The high power density fibre laser fully melts the pre-deposited powder layer according to a specific computer generated pattern. It is possible to build fine details like thin vertical walls of less than 200 µm thickness. Directly after the production process the manufactured parts or tools show a surface roughness between 10 and 20 µm Ra.

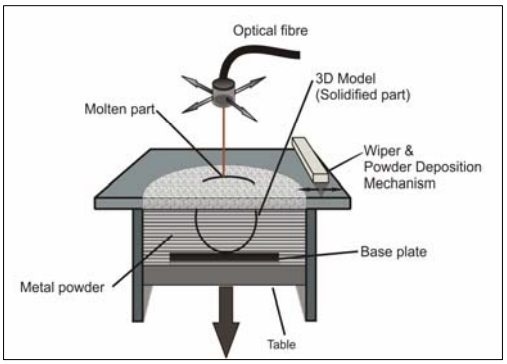

(a)

(b)

Figure 5 (a) and (b): Schematic and apparatus of SLM (MCP Realiser).

The apparatus used is the MCP Realizer, which a commercial SLM workstation with a 100 W continuous wave Ytterbium Fibre Laser (IPG, Germany) operating with a wavelength of 1068-1095 nm. The build speed is 5cm³ dense steel per hour on average, and the build envelope is 250x250x240mm. The scanning system used is a Dual Axis Mirror Positioning System (Cambridge Technology) and a Galvanometer Optical Scanner, which direct the laser beam in the x and y axis through an F-theta lens. The variable focussing optics are Sill 300 mm focal length lenses, which produce a focussed beam spot size of 60 µm diameter at 80 watts power. Since the powder is fully melted during the process, protection of the SLM-processed parts from oxidation is essential, therefore all metal powder processing occurs in an Argon atmosphere with no more than 0.2 % O_2. The build is controlled using the propriety control software Fusco.

Process parameters

Laser Power and Energy density. The results can be expressed in terms of the laser power and the dwell period (the length of exposure of the material to the beam) [Beaman et al, 1997]. For single lines, the energy density E_ρ (J/mm^2) can be expressed as:

$$E_\rho = \frac{P}{\pi r^2}\frac{2r}{v} \qquad (1)$$

where P is the Laser power (W), r the beam radius (mm) and v the scan velocity (mm/s). As it can be seen from equation (1), the laser power focused on the powder bed is of great importance to the process, however it must be taken with the other parameters in the energy density equation to give proper representation of the process. Experimental results have shown that although the same energy density E_ρ can be obtained at combinations of laser power P, scan speed V or in this case exposure time of the laser at a certain point, very different structures and properties are obtained (Lu et al. 2001). The density of the processed parts always increases as the laser energy density increases. At the same energy density, the dwell period shows the strongest influence on the density and tensile strength, the relation can be seen in Figure 6.

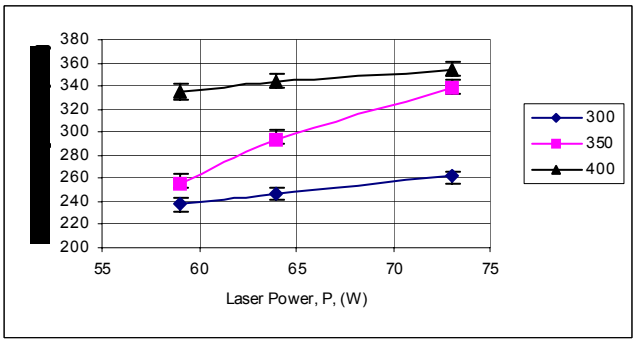

Figure 6: Tensile strength characteristics for Selective Laser Melted 316L stainless steel.

Hatch Distance. The distance between the hatch lines, i.e. the track of the laser beam, needs to be smaller than the track width so as to ensure good metallic bonding between the melted particles to yield minimum porosity. But the track width is not only determined by the laser beam size but also by the laser power, exposure time and powder property. When energy density increases, the track width becomes wider than that of the laser beam. In general, at least 30% overlap is essential to ensure good structural property [Costache et al. (2000)].

Layer thickness. The slicing of a 3D CAD model is an essential step for part fabrication with layer-based rapid manufacturing processes. The layer thickness of each slice

not only affects the quality of the finished part in the vertical-direction but also the manufacturing time. Constant layer thickness is generally used; however different layers could have different thickness according to the requirements of the part. With constant layer thickness slicing, high surface quality demands the use of thin layers in the fabrication of the part, resulting in long fabrication time. In the present work a constant 50μm layer thickness was used. Although fabrication time could be shortened with a higher value, both accuracy and surface finish of the fabricated part are degraded as layer thickness is increased [Jacobs et al. (1996)]. To obtain good metallic bonding, the track being scanned must re-melt a portion of the previous layer. Therefore the creation of the solid layer is partly from the deposited powder and partly from re-melting of the previously molten layer.

Powder characteristics. As the powder is delivered to the build platform, it is required to flow easily. Particles with smooth surfaces will move easily within the powder bed leading to a higher 'loose' density. Particle shape is also important; symmetrical particles arrange more efficiently, therefore spherical grains are preferred. These surface and granulometry parameters of the powder are closely related to the powder material and its production process. Typical powder characteristics, such as spherical particle size in the range of 20-50μm, are shown in Table 3 and the SEM image in Figure 7 shows the spherical nature of the particles [Bodycote 2003].

Table 2: Powder size distribution.

Percentage of powder in range (%)	0.2	7.4	72.0	18.3	21.0
Particle size range (μm)	45	38-45	16-38	10-16	10

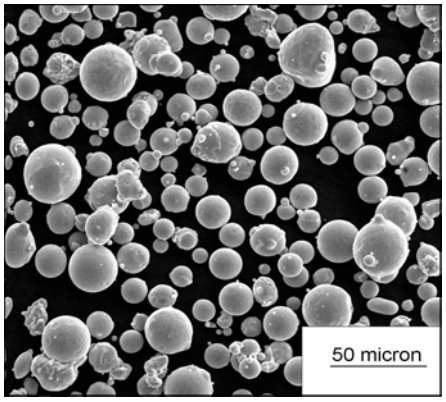

Figure 7: SEM picture of powder.

HEAT EXCHANGER TESTING

Water was chosen as the working fluid to test the performance of the micro heat exchangers and a flow loop rig was developed, shown schematically in Figure 8.

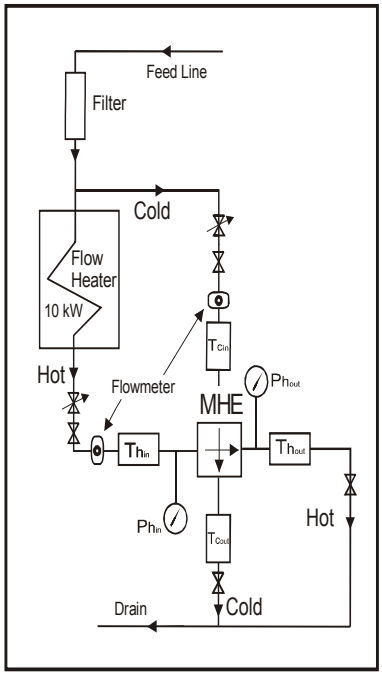

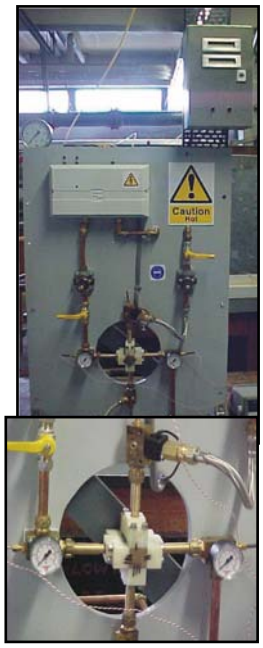

(a) (b)

Figures 8 (a) and (b): Flow loop test rig schematic.

The rig consists of connections to water tanks, a test section, Dataflow compact inline flow transmitters, platinum resistance thermometer probes, a 10 kW electric water heater and filter. The micro heat exchanger was packaged by specially designed gaskets connected to the hot and cold flow, adjacent sides of the heat exchanger were separated and sealed with epoxy, no leakage was observed. For each test, the hot and cold water flow rates, and the heat exchanger's inlet and outlet fluid temperatures were measured at steady state. The water temperatures were measured at the inlets and outlets respectively.

RESULTS AND DISCUSSION

Figure 9 shows sample micrographs of the cross sectional area of micro heat exchangers manufactured by SLM. They all have a cross-flow arrangement and provide an indication of the feature size limits, minimum channel width of 300 μm and height of 400 μm. The fin width of 150 μm shown in Figure 9 (a) represents a single laser scan line.

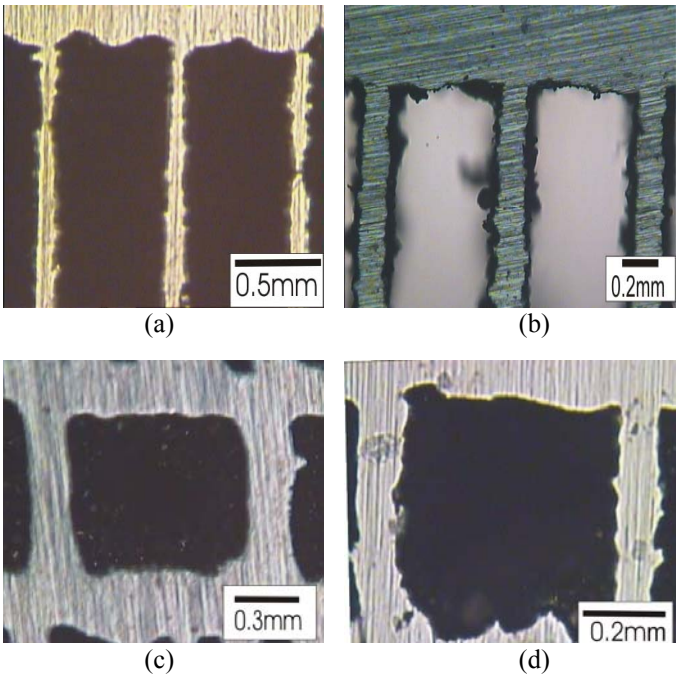

(a) (b)

(c) (d)

Figure 9 (a), (b), (c) and (d): Micrographs of micro channel heat exchangers by SLM.

The parts produced demonstrated Ra values ranging from 10 to 15 μm. The surface roughness plot of the sidewall of a heat exchanger fabricated by SLM in Figure 10 shows a large amplitude variation, explaining the dull appearance of surfaces shown in Figure 11.

The channels are clearly defined without interference; see Figure 11, which suggests the feasibility of more complex fluidic systems. This fabrication method shows great flexibility for channel geometry and offers the possibility of batch manufacturing of smart micro fluidic devices.

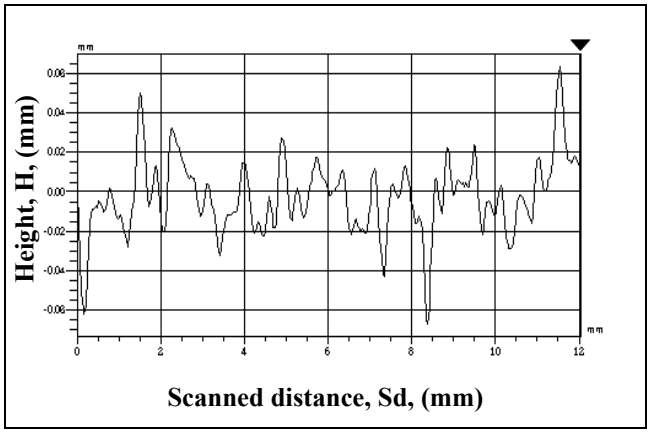

Figure 10: Roughness plot for Ra of 12 μm.

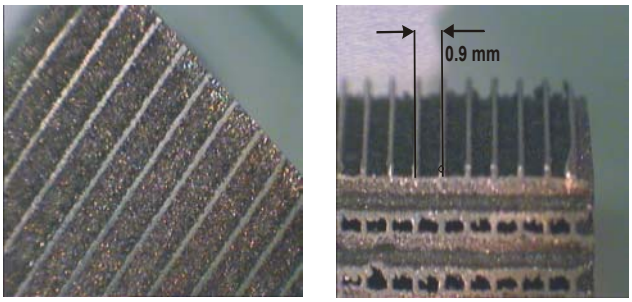

Figure 11: Frame of a typical micro cross-flow heat exchanger by SLM.

Table 3: Physical characteristics of the tested micro heat exchanger.

Structural Material	Stainless Steel 316L
Geometry	Cross flow
Channel layout	Rectangular
No. of channels per flow side	40
Hydraulic diameter, D_h	0.9 mm
Channel length, L	15 mm
Overall height	15 mm
Channel dimensions	h_c= W_c= 0.9 mm f, fin thickness = 0.1 mm Bottom thickness = 0.3 mm

Some limited experimental data for the thermal performance of an early prototype micro heat exchanger produced by SLM are presented below. The results presented have been obtained using a stainless steel micro heat exchanger with water as the working fluid. The physical characteristics of the micro heat exchanger are shown in Table 3. The data obtained in the experiments were the flow rates and inlet and outlet temperatures from both hot and cold streams. The hot-water flow rate was varied while the cold one was kept constant at its lowest value permitted by the system arrangement, (0.5 l/min). For each experimental point, the flow rates and temperatures were measured 5 times so as to determine average values.

The calculations were carried out based on a single pass, cross flow heat exchanger with both fluids unmixed [Incropera De Witt (2002)]. The heat transfer from and to the hot and cold water streams are given by:

$$Q_c = \dot{m}_c c (T_{ci} - T_{co}) \quad (2)$$

$$Q_h = \dot{m}_h c (T_{hi} - T_{ho}) \quad (3)$$

and the average heat transfer is

$$Q_{\mathrm{m}} = 0.5 \times (Q_{\mathrm{h}} + Q_{\mathrm{c}}) \tag{4}$$

Therefore the overall heat transfer coefficient, U is given by:

$$U = \frac{Q_{\mathrm{m}}}{A \times \Delta \mathrm{T}_{\mathrm{lm}}} \tag{5}$$

and the volumetric heat transfer coefficient, U_V is given by:

$$U_{\mathrm{V}} = \frac{Q_{\mathrm{m}}}{V \mathrm{F} \Delta \mathrm{T}_{\mathrm{lm}}} = U \times \mathrm{B} \tag{6}$$

where B is the ratio of total heat transfer on one side of the heat exchanger to the total volume of the heat exchanger. F is the correction factor and ΔT_{lm} is the log-mean temperature difference for a counter-flow heat exchanger, see equation 7.

$$\Delta T_{lm} = \frac{(T_{hi} - T_{co}) - (T_{ho} - T_{ci})}{\ln[(T_{hi} - T_{ho})/(T_{ho} - T_{ci})]} \tag{7}$$

In Figure 12 the overall heat transfer coefficient is calculated from the measured data as a function of the hot water flow rate. The results indicate that heat transfer performance is improving as the flow rate increases. The values of the heat transfer coefficients are not inconsistent with those found in the literature, as shown in Table 1, taken into consideration the conservative design of the heat exchanger and its large hydraulic diameter. The highest overall heat transfer coefficient was 2.22 kW/m^{2}K, which corresponds to a volumetric heat transfer coefficient of 3.14 MW/m^{3}K.

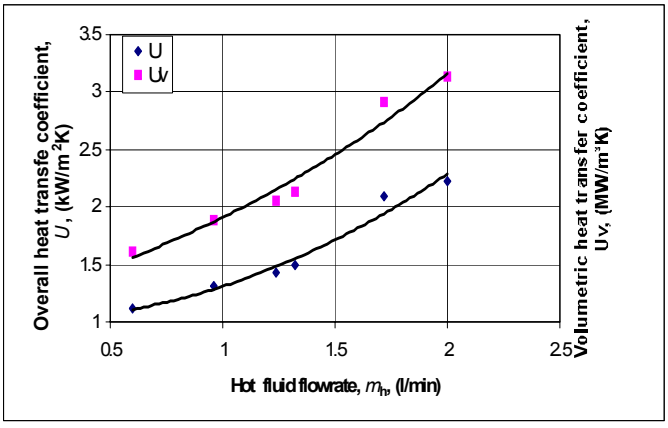

Figure 12: Overall and volumetric heat transfer coefficient as function of the hot side.

CONCLUSIONS

Microchannel heat exchangers have been fabricated using SLM, a new manufacturing technique in this application. This paper has shown the feasibility of SLM to produce microchannel heat exchanger geometries out of stainless steel.

The first device to be tested was of a very conservative design. Heat transfer and pressure drop tests need to be extended to determine and compare the performance of the devices produced with those that have been reported in the literature. Preliminary data on the structural strength of the devices has also been given, a maximum tensile strength of 350 MPa. Compared with other manufacturing processes, Selective Laser Melting offers great flexibility and the ability to produce complex channel geometries.

An experimental apparatus for measuring the performance of micro cross-flow heat exchanger has been developed in which water was used as the working fluid. Heat transfer results for the micro heat exchanger described in Table 3, showed that it was possible to achieve a volumetric heat transfer coefficient of 3.14 MW/m^{3}K and an overall heat transfer coefficient of 2.22 kW/m^{2}K, at mean logarithmic differential temperature of 36 ^{0}C with the hot water stream experiencing a pressure drop of 3 bar.

The next step in this research will be to utilize Selective Laser Melting's capabilities to produce variations in the channel geometry and flow orientation, and to investigate their effects on the heat transfer performance.

NOMENCLATURE

A	Heat exchanger transfer area on one side	**m^2**
B	Ratio of heat transfer surface area on one side to total heat exchanger volume	**m^2/m^3**
C	Heat capacity	**W/K**
C_p	Specific heat capacity of working fluid	**J/kgK**
D_h	Hydraulic diameter	**10^{-3}m**
F	Heat exchanger correction factor	
H	Height of the scanned surface	**10^{-6}m**
k_f	Thermal conductivity of working fluid	**W/mK**
$\dot{m}$	Mass flow rate	**kg/s**
P	Laser power	**W**
r	Laser beam radius	**m**
Q	Heat transfer rate	**W**
Ra	Surface roughness	**10^{-6}m**
Sd	Scanned distance of the laser sensor	**10^{-6}m**
T	Exposure time	**10^{-6}s**
TS	Tensile strength	**MPa**
U	Overall heat transfer coefficient	**W/m^{2}K**
U_V	Volumetric heat transfer coefficient	**W/m^{3}K**
ν	Scan velocity	**10^{-3}m/s**

REFERENCES

Agarwala, M., Bourell, D., Beaman, J., Marcus, H. and Barlow, J., 1995, *Rapid Prototyping J*. Vol. 1, pp. 26.

Bier, W., Keller, W., Linder, G. and Seidel, D., 1990, Manufacturing and testing of compact micro heat exchangers with high volumetric heat transfer coefficients, *Micro Structures, Sensors and Actuators*, ASME DSC 19, pp. 189-197.

Bier, W., Keller, W., Linder, G. and Seidel, D., 1993, Gas to gas heat transfer in micro heat exchangers, *Chemical Engineering and Processing*, Vol. 32, pp. 33-43.

Cross, W. T. and Ramshaw, C., 1986, Process Intensification: Laminar Flow Heat Transfer, Chemical Eng. Research and Design: *Transaction of the Institute of Chemical Engineers*, Vol. 64, pp. 258-294.

Friedrich, F. D., Kang, C. R., 1994, Micro heat exchangers by diamond machining, *Precision Eng*. 16 (1) pp. 56-59.

Kang, S.W., Chen, Y.T. and Chang, G.S., 2002, Tamkang *Journal of Science and Eng*., Vol. 5 3 pp. 129-136.

Murphy, M. L., 1995, Rapid Prototyping by Laser surface cladding, Ph. D. Thesis, Dept. of Engineering, The University of Liverpool, Liverpool, UK.

Swift, G. W., Migliori, A., Whealey, J. C., 1985, Microchannel Crossflow Fluid Heat Exchanger and Method for its Fabrication, United States Patent 4,515,632.

Tuckerman, D. B., Peace, R. F.W., 1982, High performance heat sinking for VLSI, *IEEE Electron Device Letters* EDL2 pp. 126-129.

Jiang, Pei-Xue, Fan, Ming-Hong, Guang-Shu Si, Ze-Pei Ren, 2001, Thermal-Hydraulic performance of small micro channel and porous media heat exchangers, *Int. Journal of Heat and Mass Transfer* 44, pp. 1039-1051.

Jacobs, Paul F., 1996, *Stereolithography and other RP&M Technologies*, ASME Press, New York.

Lu, L., Fuh, J. and Wong, Y. S., 2001, *Laser-Induced Materials and processes for Rapid Prototyping*, Kluwer Academic Publishers.

Bodycote Metal Technology, Test certificate 7370, 05/12/2003.

Incropera, Frank P., De Witt, David P., *Fundamentals of Heat and Mass Transfer*, 4th Edition.

Costache, F., Marian, A., Buca, D. M. and Iov, V., SIOEL '99, 6th Symp. On Optoelectronics, Ed. Teodor, Maria Robu, Dan C, Dumitras, Proc. of SPIE Vol. 4068 (2000), 555.

ACKNOWLEDGMENTS

The authors would like to thank Mr Lawrence Bailey, Mr Derek Neary and Mr Richard Arnold for their valuable contribution to the development of the research equipment.